

AN EVALUATION OF THE APPLICABILITY OF THEORETICAL  
ANALYSES TO THE FORMING LIMIT DIAGRAM

V. V. Hasek\*

INTRODUCTION

The forming limit diagram (FLD) serves as an aid to estimate the forming characteristics of sheet metals using grid line elements. With these diagrams an analysis of the plastic instabilities (necking and fracture) in the sheet metals and the determination of the limits of the forming processes are possible (Figure 1).

The term "forming limit diagram - FLD" was coined by Keeler [1] in the year 1965. He found an empirical failure criterion from a determination of the principal deformations  $\epsilon_1$  and  $\epsilon_2$  measured on the surface adjacent to failure points. Goodwin [2] extended this whole procedure for a  $\epsilon_2$  negative value of the strain .

The theoretical analysis of FLD is based on an analysis of the plastic instabilities occurring during deformation. Three schools of thought have to be differentiated here. The first theory is based on the mathematical estimation of necking occurring during sheet metal-working [3, 4, 5]. The second theory assumes that the sheet metal is non-homogeneous in thickness, the slightly lesser thickness existing at some place in the sheet metal causes necking to occur at this point, leading ultimately to failure [6]. The third theory is based on the existence of inclusions in the sheet metal, around which voids are formed during plastic deformation. When plastic deformation is sufficiently severe, the voids in the sheet metal link together, leading to fracture [8].

The present work was conducted to examine the usefulness of various theories in predicting the location and shape of the FLD. To this end, the forming limit diagram of a low-carbon steel was experimentally determined and compared with the forming limits predicted by the three theoretical approaches.

ANALYSIS OF NECKING

There are two types of necking phenomena which lead to either localized failure or diffuse necking (Figure 2). A necking zone (instability) starts building up at an angle to the direction of maximum normal stress in case of localized necking while a necking band perpendicular to the direction of maximum normal stress is formed in diffuse necking. A theoretical analysis of this problem was made by Hill [9] and Swift [3]; the type of necking was discussed by Keeler and Backofen [7] and Moore and Wallace [4].

\*Institut für Umformtechnik, Universität Stuttgart (TH), 7 Stuttgart 1, Postfach 560, West Germany.

Expressions for equivalent stress  $\bar{\sigma}$  and equivalent strain  $\bar{\epsilon}$  can be written for anisotropic material from a theory proposed by Hill [9].

$$\bar{\sigma} = \left\{ \frac{3}{2} \frac{1}{F+G+H} \left[ F(\sigma_y - \sigma_z)^2 + G(\sigma_z - \sigma_x)^2 + H(\sigma_x - \sigma_y)^2 + 2L\tau_{yx}^2 + 2M\tau_{zx}^2 + 2N\tau_{xy}^2 \right] \right\}^{1/2} \quad (1a)$$

$$d\bar{\epsilon} = \left[ \frac{2}{3}(F+G+H) \right]^{1/2} \left\{ \left[ \frac{F(Gd\epsilon_y - Hd\epsilon_z)^2 + G(Fd\epsilon_y - Hd\epsilon_z)^2 + H(Fd\epsilon_x - Gd\epsilon_y)^2}{(FG+GH+HF)^2} + \frac{2d\gamma_{zy}^2}{L} + \frac{2d\gamma_{zy}^2}{M} + \frac{2d\gamma_{xy}^2}{N} \right] \right\}^{1/2} \quad (1b)$$

where F, G, H, L, M and N are coefficients of anisotropy.

The principal strains  $\epsilon_1$  and  $\epsilon_2$  can be now calculated assuming proportional deformation and using Levy-Mises criterion as

$$\epsilon_1 = \frac{\bar{\epsilon} \left[ \left( \frac{G}{H} + 1 \right) \alpha - 1 \right]}{\left\{ \frac{2}{3} \left( \frac{F}{H} + \frac{G}{H} + 1 \right) \left[ \left( \frac{G}{H} + 1 \right) \alpha^2 - 2\alpha + \left( \frac{F}{H} + 1 \right) \right] \right\}^{1/2}} \quad (2)$$

$$\epsilon_2 = \frac{\bar{\epsilon} \left[ \left( \frac{F}{H} + 1 \right) - \alpha \right]}{\left\{ \frac{2}{3} \left( \frac{F}{H} + \frac{G}{H} + 1 \right) \left[ \left( \frac{G}{H} + 1 \right) \alpha^2 - 2\alpha + \left( \frac{F}{H} + 1 \right) \right] \right\}^{1/2}} \quad (3)$$

where  $\alpha = 1/\eta = \sigma_1/\sigma_2$ .

An exponential law of one form or other, is used to describe the relation between equivalent stress and equivalent strain

$$\bar{\sigma} = A\bar{\epsilon}^n \quad (4)$$

$$\bar{\sigma} = A_1(B_1 + \bar{\epsilon})^{n_1} \quad (5)$$

#### LOCALIZED NECKING

Hill developed the mathematical relation for the localized necking by considering velocities in the necking zone [9].

The analysis is made by assuming the flow condition and plastic potential to be identical, possessing a sixfold symmetry, and without consideration of the Bauschinger effect and the previous deformation history. The

material is subjected to uniaxial stresses only and is isotropic.

The equivalent strain for localized necking  $\bar{\epsilon}_\ell$  can be calculated, using equation (5), as

$$\bar{\epsilon}_\ell = n_1 \frac{\left\{ \frac{2}{3} \left( \frac{E}{H} + \frac{G}{H} + 1 \right) \left[ \left( \frac{G}{H} + 1 \right) \alpha^2 - 2\alpha + \left( \frac{F}{H} + 1 \right) \right] \right\}^{1/2}}{\frac{G}{H} \alpha + \frac{F}{H}} - B_1 \quad (6)$$

The principal deformation ratios  $\epsilon_{1\ell}$  and  $\epsilon_{2\ell}$  for localized necking can be obtained by substituting these values in the corresponding equations.

#### DIFFUSE NECKING

Swift [3] and Moore and Wallace [4] have analysed mathematically the instability occurring due to diffuse necking. According to Swift, necking in the tension test begins when the load on the testpiece reaches a maximum. An instability similar to the uniaxial tensile test can occur also in a testpiece subjected to biaxial stresses. This instability is of importance for deep drawing and stretching processes. The third principal stress, perpendicular to the plane of the sheet is not of great importance.

The procedure for calculating the equivalent strain in diffuse necking  $\bar{\epsilon}_d$  is the same as in the case of localized necking. The equivalent strain  $\bar{\epsilon}_d$  is determined, using equation (5), as

$$\bar{\epsilon}_d = n_1 \sqrt{\frac{2}{3} \left( \frac{F}{H} + \frac{G}{H} + 1 \right)} \frac{\left[ \left( 1 + \frac{G}{H} \right) \alpha^2 - 2\alpha + \left( 1 + \frac{F}{H} \right) \right]^{1/2}}{\left( 1 + \frac{G}{H} \right)^2 \alpha^3 - \left( 1 + \frac{2G}{H} \right) \alpha^2 - \left( 1 + \frac{2F}{H} \right) \alpha + \left( 1 + \frac{F}{H} \right)^2} - B_1 \quad (7)$$

The principal strains  $\epsilon_{1d}$  and  $\epsilon_{2d}$  for diffuse necking can then be obtained from the corresponding equations.

Computer programmes were developed to determine the stress and strain relations using the equations derived from both localized and diffuse necking, and their limits ( $\epsilon_\ell$ ,  $\epsilon_d$ ) are shown in Figure 5.

#### THEORY BASED IN THE INHOMOGENEITY OF THE MATERIAL (MARCINIAK [6])

In this theory the material is assumed to be initially inhomogeneous. The local instability occurs first at points of inhomogeneity and a local necking zone is created. This necking zone will be perpendicular to the maximum normal stress.

Figure 3 shows an element in a sheet metal with an initial homogeneity, and the stresses acting on it. This inhomogeneity in the sheet metal need not necessarily be due to a smaller thickness but can have other causes such as porosity.

The initial inhomogeneity  $T_0$  is defined as

$$T_0 = \left( \frac{s_B}{s_A} \right) \quad (8)$$

where  $s_A$  and  $s_B$  are the sheet hardness outside and in the groove, respectively.

The initial inhomogeneity is normally difficult to determine. Therefore a value of  $T_0 = 0.98$  is generally and arbitrarily assumed. If such a sheet metal is deformed, both the necking zone B and the surrounding area A expand till fracture occurs in zone B. Marciniak [6] has proposed a theory to describe the critical strains in region A, assuming that Hill's theory for anisotropic materials is valid, the flow curve of the material can be described by the equation proposed by Swift [3], and that the Levy-Mises relations can be used to anisotropic materials. The equivalent stress is defined as:

$$\bar{\sigma} = \frac{\sqrt{3}}{2\sqrt{(2R+1)}} [(R+1)\sigma_1^2 + (R+1)\sigma_2^2 - 2R\sigma_1\sigma_2] \quad (9)$$

where  $R$  is the normal anisotropy ratio.

The force equilibrium equation perpendicular to zone B is given by Figure 3

$$\sigma_{1B} \cdot s_B = \sigma_{1A} \cdot s_A \quad (10)$$

At the onset of necking in zone B a plane strain ( $d\epsilon_2 = 0$ ) is created. An internal stress parameter  $u$  can be defined as

$$u = \frac{\sigma_{1B}}{\bar{\sigma}_B} \cdot \frac{\sqrt{3(2R+1)}}{\sqrt{2(R+1)}} \quad (11)$$

The value of  $u$  determines the stress condition in region B. Plane strain condition exists for  $u = 1$ . For a known stress ratio  $\psi$ , for which a corresponding strain ratio  $\alpha$  exists, an equation for  $u$  is now derived. The expressions defining  $\sigma_{1B}$  and  $\bar{\sigma}_B$  are substituted in equation (11) and the following equation is obtained after simplifications.

$$\frac{du}{u} = \left[ \frac{1}{A+B\epsilon_2} + \left( C \cdot u - \frac{1}{D+B \int \frac{d\epsilon_2}{\sqrt{1-u^2}}} \right) \frac{1}{\sqrt{1-u^2}} + E \right] \quad (12)$$

where  $A$ ,  $B$ ,  $C$ ,  $D$  and  $E$  are constants.

From equation (12) the following equation is obtained

$$\bar{\epsilon}_A = \frac{2\sqrt{1/2(R+1)\psi^2 + \psi + 1}}{\sqrt{3(2R+1)}} \cdot \epsilon_2 \quad (13)$$

$\psi$  is calculated from  $\alpha$  as follows:

$$\psi = \frac{\epsilon_{3A}}{\epsilon_{2A}} = \frac{-\alpha - 1}{(R+1) - R\alpha} \quad (14)$$

Using equation (12) again, we get  $\epsilon_{1A}$  and  $\epsilon_{2A}$ .

$$\epsilon_{1A} = \frac{(R+1)\alpha - R}{2\sqrt{(2R+1)/3}} \cdot \bar{\epsilon}_A \quad (15)$$

$$\text{and } \epsilon_{2A} = \frac{(R+1) - R\alpha}{2\sqrt{(2R+1)/3}} \cdot \bar{\epsilon}_A \quad (16)$$

The set of equations is difficult to programme and computing consumes a lot of time. The forming limit from this inhomogeneity theory (M) is shown in Figure 5.

#### THEORY BASED ON THE INCLUSION OF THE MATERIAL (GOSH [8, 11])

The fracture criterion for this theory was proposed by McClintock [10], who modeled the process of initiation, growth and coalescence of voids. Although voids can initiate from intersection shear bands in a pure metal, in most ductile metals void initiation takes place either by separation of included particles from the matrix or by cracking of inclusions. This happens rather early during deformation and considerable additional plastic flow is taking place before fracture. The process of shear joining of growing voids in sheets is shown schematically in Figure 4.

The formulation of a criterion for sheet forming applications is then based on this stress-dependent criterion [10]:

$$(1+\eta)\sigma_1^2 = K \quad (17)$$

The principal strains at fracture may now be calculated from conventional plasticity theory. Relations from Hill's theory of anisotropic plasticity [9] are used for this purpose with an assumption of proportional straining of sheets.

The principal strains at fracture are defined as

$$\epsilon_1 = \frac{[A'^2 K (1+\eta - P'\eta) / C^2 (1+\eta)]^{1/2n}}{n' (1+\alpha^2 + P'\alpha)^{1/2}} \quad (18)$$

$$\epsilon_2 = \epsilon_1 \alpha$$

where  $A'$ ,  $B'$  and  $P'$  are constants.

This is valid if  $A$ ,  $n$ ,  $R$  and  $K$  are known;  $\epsilon_1$  and  $\epsilon_2$  can be determined.

For the determination of these strains, computer programmes were developed and the resulting forming limit is shown in Figure 5 (the curve G).

#### COMPARISON OF THEORIES WITH THE EXPERIMENTAL FLD

As will be seen from Figure 5 all the three theories of necking in sheet metal-working under biaxial stress conditions give curves that are lower than the experimentally determined one.

The theory based on initial inhomogeneity (M) and the theory based on inclusions (G) show greater deviation from the experimental values in the second strain quadrant ( $\epsilon_1, \epsilon_2$ ) than the values computed from the necking theory ( $\epsilon_d$ ). This arises from the difficulty of choosing a proper value for  $T_0$  for the inhomogeneity theory and from the assumption that all active inclusions are spherical according to the inclusion theory. In addition, the values of  $R$ ,  $N$  and  $B_1$  need be determined to a very high accuracy. The smallest discrepancy between experimental and theoretical curves in the first quadrant ( $\epsilon_1, -\epsilon_2$ ) is shown by the theory based on inclusions (G).

In judging the suitability of various theories, it should also be considered that the equations of the necking and the inclusion theories can be solved without much difficulty. On the other hand this process is difficult for the inhomogeneity theory, and the complicated differential equation (12) is particularly hard to solve. The necking theories and the inclusion theory cover the whole region of ideal drawing ( $\epsilon_1 = -\epsilon_2$ ) up to ideal stretch drawing ( $\epsilon_1 = \epsilon_2$ ). The inhomogeneity theory considers only the region on positive strain (from  $\epsilon_2 = 0$  to  $\epsilon_1 = \epsilon_2$ ).

In conclusion, the various mathematical theories of necking offer some insight into the possible mechanisms of necking, without eliminating the need for the determination of forming limit diagrams.

#### REFERENCES

1. KEELER, S. P., SAE Paper 650535, 1965.
2. GOODWIN, G. M., SAE Paper 680093, 1968.
3. SWIFT, H. W., J. Mech. Phys. Solids 1, 1952, 1.
4. MOORE, G. and WALLACE, J., Inst. Metals 93, 1964/65, 33.
5. HASEK, V., Berichte aus dem Institut für Umformtechnik, 25, Stuttgart, 1973.
6. MARCINIAK, Z., KUCZYNSKI, K. and POKORA, T., Int. J. Mech. Sci. 15, 1973, 789.
7. KEELER, S. P. and BACKOFEN, A., Trans. ASM 56, 1963, 25.
8. GOSH, A. K., Met. Trans. 7A, 1976, 533.
9. HILL, R., "The Mathematical Theory of Plasticity", Oxford University Press, 1971.
10. McCLINTOCK, F. A., J. Appl. Mech. 35, 1968, 363.
11. GOSH, A. K. and HECKER, S. S., 2nd North American Metalworking Conference, Madison, 1974.

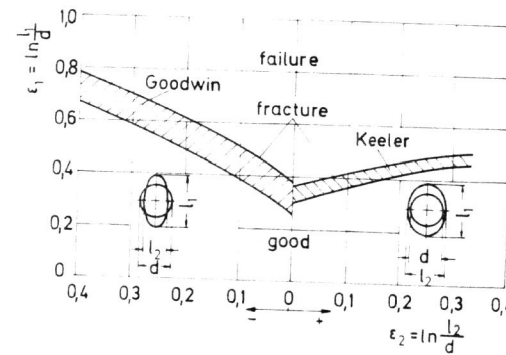


Figure 1 Forming Limit Diagram

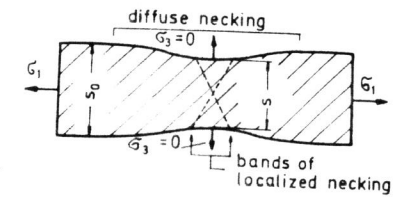


Figure 2 Localized Necking in the Region of Diffuse Necking

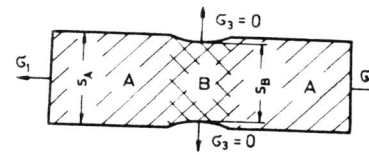


Figure 3 Sheet Metal Element Showing Inhomogeneity

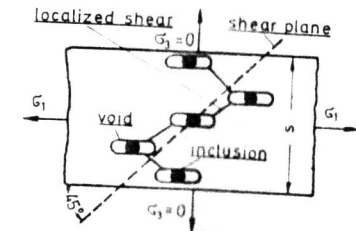


Figure 4 Illustration of Sheet Metal Elements Containing Inclusions and Voids

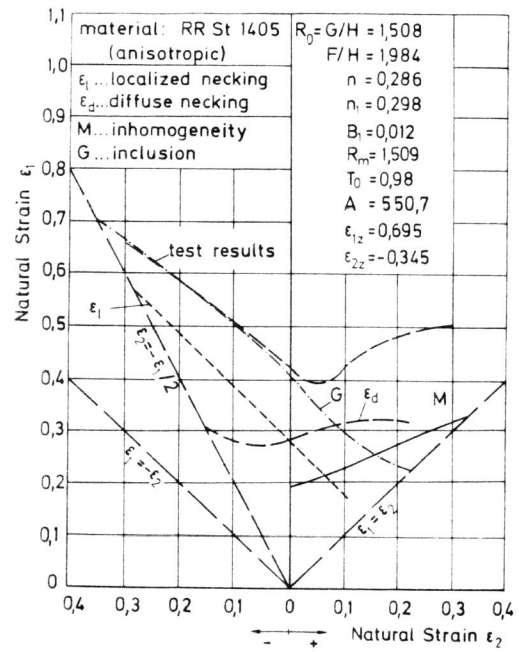


Figure 5 Comparison of Theoretical Limit Curves with Experimental Curves